Am J Transl Res 2022;14(5):3360-3371
www.ajtr.org /ISSN:1943-8141/AJTR0141250

Original Article

Interaction between COX-2 and ER stress is involved in the apoptosis-induced myocardial ischemia/reperfusion injury

Wenhui Tao[1,2*], Lingui Li[1,2*], Junkai Hu[1,2*], Shangxian Xu[1], Biying Wang[1], Jun Ding[1], Mian Zhang[1,2], Xiaowen Meng[1,2], Xiang Wei[1], Xisheng Shan[1,2], Ke Peng[1,2], Huayue Liu[1,2], Fuhai Ji[1,2]

[1]Department of Anesthesiology, First Affiliated Hospital of Soochow University, Suzhou, Jiangsu, China; [2]Institute of Anesthesiology, Soochow University, Suzhou, Jiangsu, China. [*]Equal contributors.

Received December 21, 2021; Accepted March 31, 2022; Epub May 15, 2022; Published May 30, 2022

Abstract: Purpose: Apoptosis induced by excessive endoplasmic reticulum (ER) stress is accompanied by the occurrence and progression of myocardial ischemia/reperfusion (I/R) injury. COX-2 is also known to affect the development of I/R damage in myocardium. However, the interaction between COX-2 and ER stress in aggravating myocardial I/R lesion is not well characterized. Therefore, the purpose of our research was to explore the interaction between COX-2 and ER stress on myocardial apoptosis. Methods: The left anterior descending (LAD) coronary artery was ligatured with a 6-0# suture for 0.5 hours and subsequently subjected to reperfusion for 3 hours to simulate myocardial I/R in mice. Oxygen glucose deprivation/reoxygenation (OGD/R) was performed on H9c2 cells to construct an in vitro model of this experiment. NS398 (COX-2 specific inhibitor) and Salubrinal (Sal, ER stress inhibitor) were administered to assess the function of COX-2 and ER stress in myocardial I/R impairment. CCK-8 assay was used to evaluate the viability of H9c2 cells under different treatment conditions. TUNEL and Hoechst staining were used to detect the occurrence of apoptosis. Infarct area/area at risk and Hematoxylin-eosin stained sections were assessed after I/R. Protein expressions of glucose-regulated protein 78 (GRP78), COX-2, phosphorylation of eukaryotic translation initiation factor 2 alpha (p-eIF2α), CCAAT/enhancer-binding protein homologous protein (CHOP), and Cleaved caspase 3 in the myocardium were examined using Western blotting. Changes in Cleaved caspase 3 expression in myocardial slices were measured by immunohistochemistry. Results: Sal or NS398 partly reduced I/R-induced damage as testified by the apparent decrease in infarct size after I/R and reduced cell viability following OGD/R. Sal distinctly increased p-eIF2α, but caused decreased expression of COX-2, Cleaved caspase 3, and ER stress-associated proteins after I/R, suggesting that Sal effectively inhibited ER stress, apoptosis, and COX-2. Pretreatment with NS398 blocked I/R or OGD/R-induced upregulation of COX-2, Cleaved caspase 3, and ER stress-related marker proteins. Conclusions: Interaction of COX-2 and ER stress regulates apoptosis and contributes to Myocardial lesion induced by I/R.

Keywords: Ischemia/reperfusion, cyclooxygenase-2, apoptosis, oxygen-glucose deprivation/reoxygenation, endoplasmic reticulum stress

Introduction

Acute myocardial injury (AMI) is characterized by ischemia/reperfusion (I/R)-induced cardiomyocyte apoptosis, which is a complex pathophysiological phenomenon. In clinical settings, the high incidence and mortality rate of AMI patients was mainly due to I/R damage [1, 2]. Previous studies have demonstrated the association of myocardial I/R impairment with inflammatory response [3, 4], oxidative stress [5, 6], cardiomyocyte death [7, 8], and mitochondrial dysfunction [9, 10]. Apoptosis was a pathophysiological process following I/R, which aggravated the myocardial impairment [11, 12]. Although the secondary myocardial damage induced by I/R is well documented, there is a paucity of therapeutic target modalities for I/R.

Studies have shown that COX-2 promotes cardiomyocyte damage since it was a critical mediator of inflammation, apoptosis, and septic shock, leading to evident lesion [13]. However,

a study of 2586 patients treated with rofecoxib showed twice the risk of heart attack or stroke compard with patients treated with placebo [14, 15]. It is not clear yet why certain COX-2 inhibitors increase the risk of cardiovascular events. Recently, it has become increasingly convincing that Endoplasmic Reticulum (ER) stress is conducive to cell adaptation and is a self-protection mechanism [16]. However, excessive and sustained ER stress induced by I/R promoted cell death, which would affect the progression of myocardial damage. Inhibition of ER stress-induced apoptosis is a known therapeutic target for myocardial damage [17-19]. Salubrinal (Sal), a selective phosphatase inhibitor of p-eIF2α, was shown to ameliorate diabetes' myocardial damage by inhibition of ER stress and ferroptosis [20]. However, the underlying molecular mechanisms by which Sal alleviates apoptosis after myocardial I/R are remain elusive.

The specific COX-2 inhibitor parecoxib has been implicated roles in regulation of ER stress-mediated apoptosis of nucleus pulposus cells [21]. However, whether COX-2 is involved in modulating ER stress in myocardial I/R remains unclarified. Reducing the expression of marker proteins in the ER stress and mitigating I/R-induced apoptosis has demonstrated the cardioprotection effect of NS398. In addition, ER stress has been shown to promote the expression of COX-2 via ATF4 [22, 23]. Therefore, we hypothesized that the effects of COX-2 inhibitor on myocardial damage and apoptosis induced by I/R may be partly attributed to their interaction with ER stress. To test this hypothesis, we investigated the effects of NS398 and Salubrinal on ER stress and COX-2 in mice and H9c2 cells.

Materials and methods

Drugs and reagents

Cell Counting Kit-8 (K1018, ApexBio, USA), LDH kit (A020-2-2, Jiancheng, China), and Hoechst 33258 (C1017, Beyotime, China) were purchased. Salubrinal (SML0951, Sigma-Aldrich, USA), a specific inhibitor of ER stress [24, 25], which could reduce myocardial damage induced by I/R [20]. NS398 (HY-13913, MedChemEXpress, USA), an inhibitor of COX-2 [26, 27], has been utilized to evaluated hypoxia/reoxygenation-induced cardiomyocyte apoptosis [28].

Ethics statement

The study protocol was ratified by the Animal Ethics Committee of First Affiliated Hospital of Soochow University (No. 2018-043).

Animals and groups

C57BL mice (age: 7-8 weeks; weight: 18-22 g) were purchased from Cavens Biogle animal Co. Ltd. (Soochow, China). Mice fed in isolated cages in a controlled environment and were acclimatized for 1 week before the experiment. Mouse myocardial damage model constructed by I/R treatment was as formulated in the previous experiments [29, 30]. In brief, cut along the left edge of the sternum to find the mouse heart. Ligation of the LAD under the microscope. Ischemia was evidenced by the appearance of the pale color of the tip of the heart and typical S-T segment elevation on the electrocardiogram. The ligature was cut after 30 min of ischemia to restore blood flow of the coronary artery. Successful reperfusion was indicated by the restoration of red color of the anterior wall of the left ventricle and decline in the ST-segment on the electrocardiogram. Reperfusion was maintained for 3 h.

The following four groups were established in our study: (1) Sham group (threading only); (2) I/R group; (3) I/R+Sal group (mice were administered intraperitoneal injection of Salubrinal 1 mg/kg 0.5 h before ligation [31, 32]); (4) I/R+NS398 group (mice were administered intraperitoneal injection of NS398 5 mg/kg 0.5 h before ligation [33]). Pentobarbital was used to anesthetize mice (45 mg/kg, intraperitoneal injection). Damage phenotypes were assessed by Evans Blue & TTC staining and H&E staining. Apoptosis detected by Western blot and TUNEL staining.

H9c2 culture and OGD/R establishing

H9c2 cells were cultured in Dulbecco modified Eagle medium (DMEM) containing 10% fetal bovine serum (FBS) and 1% mycillin. Set the temperature in the incubator to 37°C and maintain CO_2 concentration at 5%. The model construction of oxygen-glucose deprivation/reoxygenation (OGD/R) refers to previous stud-

ies [34, 35]. Briefly, H9c2 cells were cultured in glucose-free DMEM and in a 37°C bell jar filled with N_2 and CO_2 (95%: 5%) for 6 h. Subsequently, the cells were cultured under normoxia for another 6 h.

The following four treatments were established: (1) Control; (2) OGD/R treatment; (3) OGD/R+Sal treatment (H9c2 disposed by Salubrinal 20 μM for 6 h before OGD/R [36]); (4) OGD/R+NS398 treatment (H9c2 disposed by NS398 10 μM for 1 h before OGD/R [37]). All agents were added to the changed medium during OGD/R stimulation to maintain the working concentration.

Hematoxylin-eosin (H&E) staining and immunohistochemistry

The detailed procedure used for H&E staining is described elsewhere [34]. Briefly, freshly harvested myocardial tissues first subjected to 4% paraformaldehyde-fixed. The tissue was embedded in paraffin and then sliced with a thickness of about 5 μm to be stained with hematoxylin and eosin and observed by light microscopy (Nikon, Japan).

Evans blue and TTC staining

Animals were anesthetized, the LAD artery was re-occluded and Evans blue dye (2%) was injected through the inferior vena cava. The tissue samples were collected, frozen and cut to a thickness of 2 mm, which were immersed in TTC solution (2, 3, 5-tri-phenyltetrazolium, 1%) in 37°C normal saline for 0.5 h and then photographed. The unstained area was calculated using the Image J software.

Western blot analysis

Extract the total proteins in myocardium or cells with PMSF and RIPA, and carefully detect the proteins concentration through protein analysis kit (P0012, Beyotime, China). The PVDF membrane (Millipore, Bedford, USA, containing proteins) was sealed with 5% skimmed milk at room temperature for 2 h. After rinsing, the primary antibody was added and incubated overnight at 4°C: GRP78 (C50B12), p-eIF2α (D9G8), eIF2α (D7D3), CHOP (L63F7), cleaved caspase 3 (Asp175). The dilution ratio of antibodies above was 1:1000 and purchased from Cell Signaling Technology (USA). β-tubulin (1:3000, C66, Abmart, China), COX-2 (1:1000, ab62331, Abcam, USA).

CCK-8 and lactate dehydrogenase assay

The prepared cell suspension was transferred to the 96-well plate (6×10^3 cells/100 μl per well). Different treatments will be given after the cells were adhered. Only DMEM was added in the control group. Each group had five duplicate holes. The optical density value was detected by Spectra Max 190 plate reader under the condition of the 450 nm wavelength.

TUNEL staining

For the quantification of cardiomyocyte apoptosis, TUNEL staining (C1086, Beyotime, China) was performed in line with the specification. The fluorescence intensity was observed under a fluorescence Microscope (DM1000, Leica, USA).

Hoechst staining

Cells were fixed with 4% formaldehyde (room temperature, 10 min), rinsed thrice with phosphate-buffered saline, and incubated with 20 mM Hoechst 33258 (C1017, Beyotime, China) in dark for 10 min. Typical apoptotic cells with bright blue nuclei, pyknosis, and fragmentation could be observed under a fluorescence microscope (ECLIPSE Ts2R-FL, Nikon, Japan).

Statistical analysis

Graphpad 8.0 was used for data statistics and picturing. Continuous variables were expressed as mean ± standard deviation, and the differences between the two groups were evaluated by independent-samples T test. More than three groups require the use of one-one ANOVA with post hoc pairwise test. Two-tailed, *P* values <0.05 were considered statistically significant.

Results

COX-2 and cleaved caspase 3 were elevated in OGD/R H9c2 and in I/R myocardium

As I/R injury is primarily on account of OGD/R, H9c2 cells were treated with OGD/R as an in vitro cell model of myocardial damage. LDH release increased following OGD/R treatment

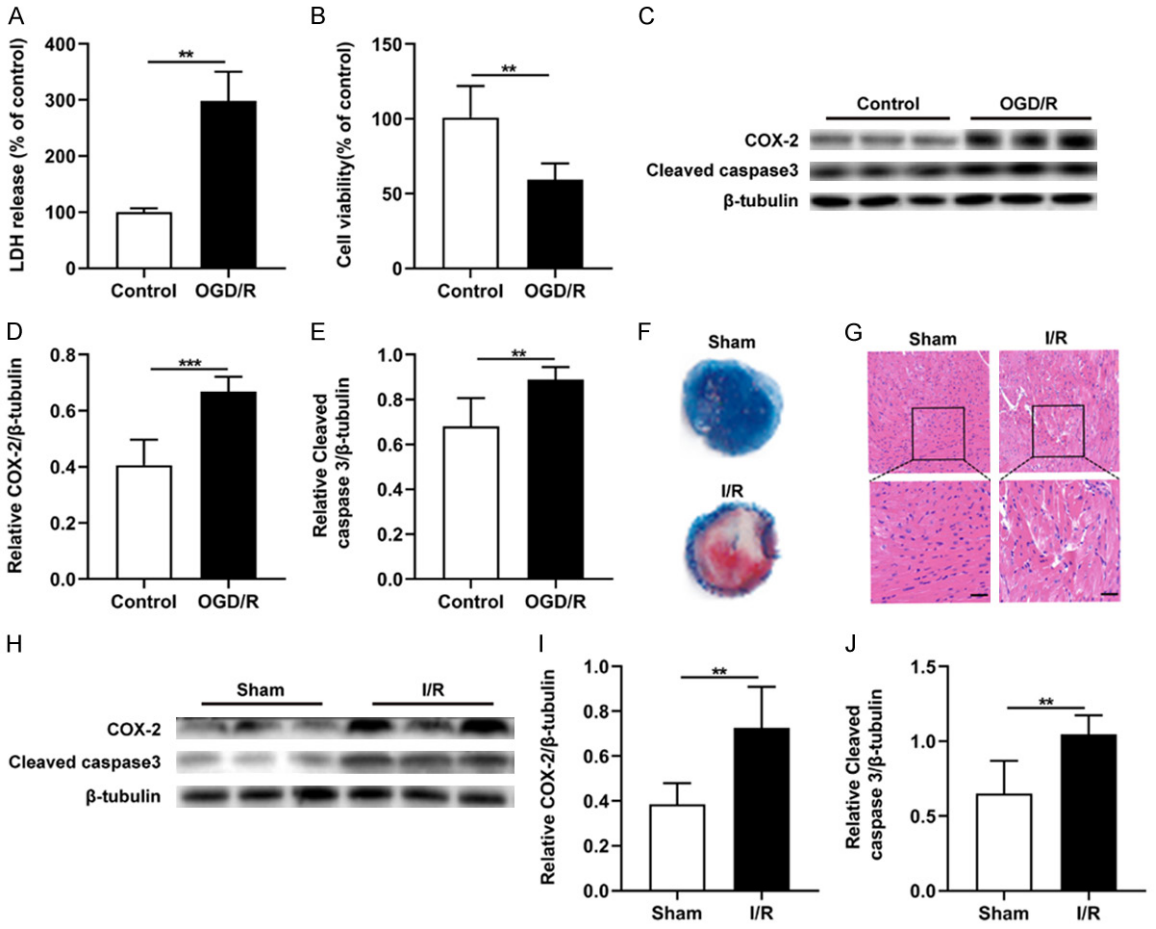

Figure 1. Involvement of COX-2 in OGD/R or I/R-induced apoptosis and damage. A, B. LDH release and cell viability in the supernatant (n=5). C-E. Western blot analysis of COX-2 and Cleaved caspase 3 protein expressions in H9c2 cells (n=6). F. Evans blue and TTC staining of heart section. G. Representative images of H&E-stained sections (scale bar =50 μm). H-J. Western blot analysis of COX-2 and Cleaved caspase 3 in the myocardial tissue (n=6). Data shown as mean ± standard deviation. **P<0.01, ***P<0.001.

(**Figure 1A**), and cell viability decreased detected by CCK-8 assay (**Figure 1B**). The expression of COX-2 and Cleaved caspase 3 increased significantly in the OGD/R group rather than in the control group (**Figure 1C-E**). In vivo, the I/R treatment significantly enhanced the myocardial infarct (**Figure 1F**). And mice with I/R showed enhanced bleeding and neutrophil infiltration, irregular and disordered arrangement of myocardial bundles (**Figure 1G**). The expressions of COX-2 and Cleaved caspase 3 induced in I/R myocardium compared with that in normal myocardium (**Figure 1H-J**), which was consistent with the conclusion of in vitro experiment. These findings indicated the potential involvement of COX-2 in I/R or OGD/R-induced apoptosis and damage.

ER stress was present in H9c2 OGD/R and myocardial I/R

GRP78, p-eIF2α, and CHOP, are recognized to play a pivotal role in ER stress regulation. As shown in **Figure 2**, GRP78, p-eIF2α, and CHOP in the OGD/R group were distinctly higher than those of the control group (**Figure 2A-D**). Consistent with the in vitro results, GRP78, p-eIF2α, and CHOP were induced in I/R mice compared with that in Sham mice (**Figure 2E-H**).

Sal attenuated apoptosis and injury by inhibiting ER stress-mediated COX-2 signaling pathway in vitro and in vivo

To further pursue the relationship during ER stress, COX-2, apoptosis, and injury, Sal was

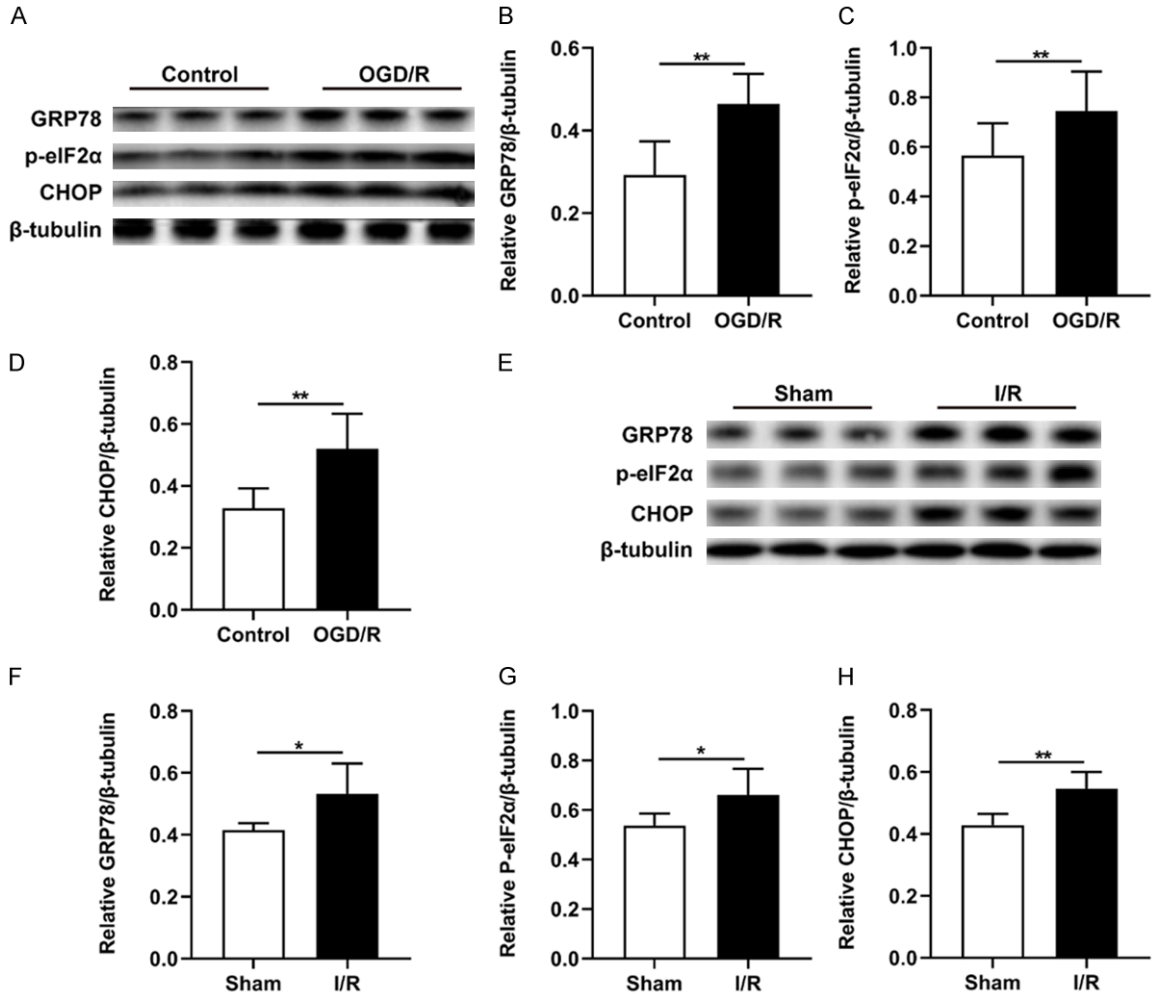

Figure 2. ER stress was present in H9c2 OGD/R and myocardial I/R. A-D. Results of Western blot analysis showing protein expressions of GRP78, p-eIF2α, and CHOP in H9c2 cells (n=6). E-H. Western blot analysis of GRP78, p-eIF2α, and CHOP proteins in the myocardial tissue (n=6). Data presented as mean ± standard deviation. *P<0.05, **P<0.01.

used. Results of CCK-8 assay showed that pretreatment with Sal increased cell viability (**Figure 3A**), and significantly decreased LDH release (**Figure 3B**). Hoechst staining showed the typical morphological characteristics of apoptosis in OGD/R cells. Pretreatment with Sal was found to attenuate cell apoptosis following OGD/R (**Figure 3C**, **3D**). In addition, p-eIF2α was examined as an indicator of I/R-induced ER stress in the myocardium after Sal administration, Western blot showed that Sal distinctly suppressed the dephosphorylation of p-eIF2α after OGD/R. The level of GRP78, COX-2, CHOP, and Cleaved caspase 3 were markedly reduced in the OGD/R+Sal-treated group compared with the OGD/R group (**Figure 3E**, **3F**). Our results manifested that Sal effectually restrained ER stress, COX-2, and apoptosis.

In vivo, mice were treated with Sal and then subjected to I/R. Sal pretreatment was found to significantly reduce the infarct area/area at risk (**Figure 4A**, **4B**). Immunohistochemistry (IHC) also confirmed that Sal reduced the expression of Cleaved caspase 3 in myocardial tissue (**Figure 4C**, **4D**). Consistently, TUNEL assay showed that enhanced apoptosis following I/R was inhibited by Sal administration (**Figure 4E**, **4F**), indicating that Sal ameliorated myocardial apoptosis. Sal markedly mitigated the structural impairment of myocardium

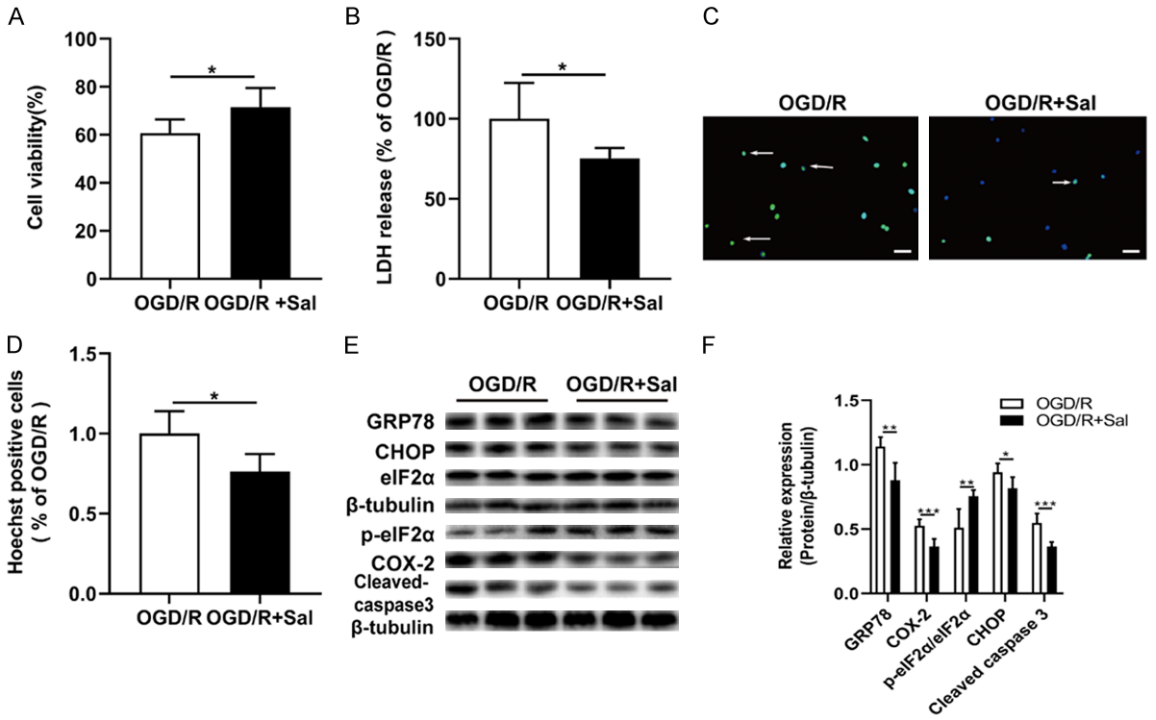

Figure 3. Sal attenuated apoptosis and injury by inhibiting ER stress-mediated COX-2 signaling pathway in vitro. A. Results of CCK-8 assay (n=5); B. Lactate dehydrogenase activity (LDH) (n=5); C, D. Hoechst 33258-stained sections showing apoptotic cells (white arrows) (n=5, Scale bar: 50 μm). E, F. Western blot analysis of GRP78, CHOP, eIF2α, p-eIF2α, COX-2, and Cleaved caspase 3 proteins in H9c2 cells (n=6). Data presented as mean ± standard deviation. $^{*}P<0.05$, $^{**}P<0.01$, $^{***}P<0.001$.

(**Figure 4G**). In addition, Sal induced p-eIF2α expression and reduced the expressions of Cleaved caspase 3, COX-2, and ER stress-related proteins (**Figure 4H**, **4I**). Collectively, our results indicated the involvement of ER stress in apoptosis-induced myocardial damage and suggested that Sal protects against myocardial I/R injury by inhibiting ER stress-mediated COX-2 signaling pathway.

NS398 decreases ER stress-induced apoptosis following OGD/R by inhibiting COX-2 in vitro

To assess whether ER stress is also a mediator of the effects of COX-2 in I/R damage, NS398-pretreated OGD/R H9c2 cells. Results of CCK-8 test revealed that NS398 decreased cell death (**Figure 5A**). Preconditioning with NS398 alleviated cell apoptosis (**Figure 5B**, **5C**) and decreased LDH release (**Figure 5D**) following OGD/R. Moreover, NS398 pretreatment of H9c2 cells significantly decreased the proteins level of GRP78, Cleaved caspase 3, COX-2, and CHOP (**Figure 5E**, **5F**).

NS398 alleviates ER stress-induced apoptosis following myocardial I/R by suppressing COX-2

We further used NS398 to probe the interaction between COX-2 and ER stress in myocardial I/R. Results of TUNEL assay showed that NS398 treatment dampened the enhanced apoptosis after I/R (**Figure 6A**, **6B**). Pretreatment with NS398 markedly reduced the myocardial infarct size caused by I/R (**Figure 6C**, **6D**). Immunohistochemistry also confirmed that NS398 reduced the expression of Cleaved caspase 3 in myocardial tissue (**Figure 6E**, **6F**). NS398 markedly mitigated the structural damage of myocardial tissue (**Figure 6G**). Consistent with the experimental results in vitro, the proteins levels of GRP78, CHOP, Cleaved caspase 3, COX-2 were significantly decreased by NS398 pretreatment *in vivo* (**Figure 6H**, **6I**). These data demonstrated that NS398 alleviates myocardial I/R-induced apoptosis through regulating COX-2/ERS signaling pathway.

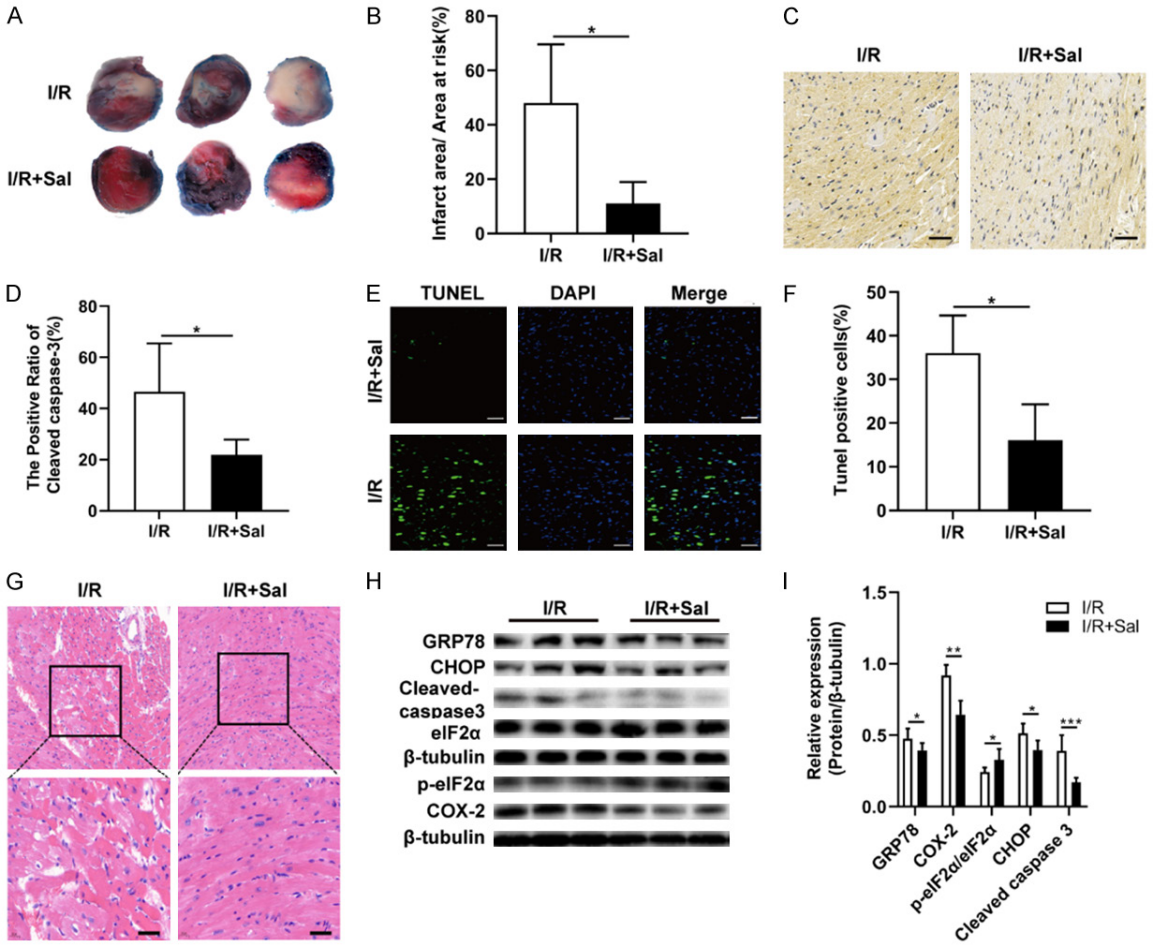

Figure 4. Sal attenuated apoptosis and injury through inhibiting ERS-mediated COX-2 signaling pathway in vivo. A, B. Evans blue and TTC staining (n=3); C, D. Immunohistochemistry (IHC) (n=4), Scale bar: 50 μm; E, F. TUNEL assay, (n=4), Scale bar: 50 μm; G. HE-stained heart section (n=4), Scale bar: 50 μm; H, I. Western blot analysis of GRP78, CHOP, Cleaved caspase 3, eIF2α, p-eIF2α, and COX-2 proteins in myocardial tissue (n=6). Data presented as mean ± standard deviation. *P<0.05, **P<0.01, ***P<0.001.

Discussion

In this research, we explored whether the coactions between ER stress and COX-2 are involved in the myocardial I/R-induced damage and apoptosis. Suppression of ER stress or COX-2 partly alleviated myocardial damage and apoptosis. Our data indicate the involvement of the interaction between COX-2 and ER stress in the apoptosis-induced myocardial I/R injury.

ER stress has been confirmed to be associated with the progression of I/R [38], and to contribute to the activation of apoptosis [39]. GRP78, CHOP, and p-eIF2α are all recognized indices proteins of ER stress [16]. Our results showed markedly increased ER stress marker proteins, indicating the reaction of ER stress in mice with I/R. To ascertain the function of ER stress in the myocardial elicited by I/R, Sal was used in a mouse model of I/R injury.

Sal is a specific phosphatase inhibitor of p-eIF2α. In our study, Sal markedly suppressed the dephosphorylation of eIF2α following myocardial I/R, and reduced ER stress-associated proteins. The eIF2α signaling pathway is critical for adaptation to ER stress, improving the ability of folding and restoring translation of ER [16]. Our results demonstrated increase of p-eIF2α after I/R, which might be correlated with promotion of cell survival. Nevertheless, uncontrolled activation of CHOP after myocardial I/R revealed persistent and severe I/R, and thus resulted in the activation of ER stress. The protein expression of Cleaved capase3

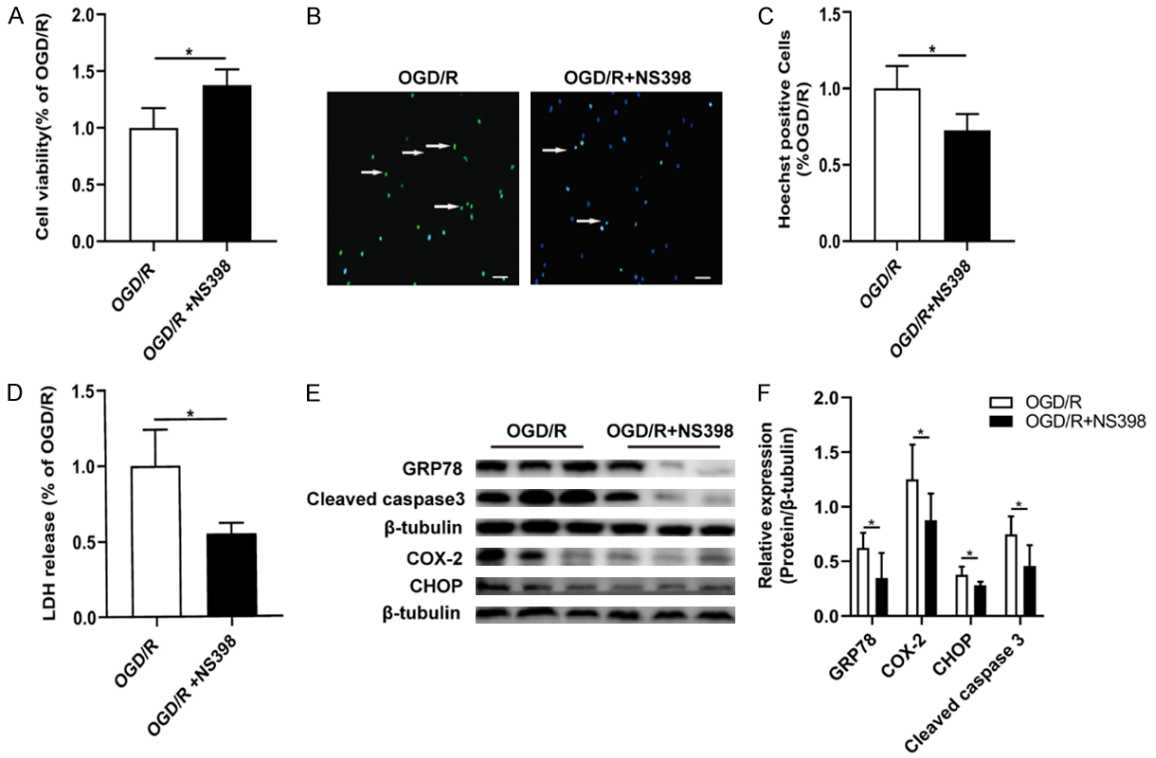

Figure 5. NS398 decreased ER stress-induced apoptosis following OGD/R through inhibition of COX-2 in vitro. A. CCK-8 assay (n=5); B, C. Hoechst 33258 staining showing the apoptotic cells (white arrows) (n=5), Scale bar: 50 μm; D. Lactate dehydrogenase activity (LDH) (n=5); E, F. Western blot analysis of GRP78, Cleaved caspase 3, COX-2, and CHOP proteins in H9c2 cells (n=6). Data presented as mean ± standard deviation. *P<0.05.

was examined so as to evaluate I/R-mediated apoptosis. The results also showed upregulation of Cleaved capase3 expression and increased infarct area in the I/R group, which was reversed by Sal pretreatment, suggesting that Sal could block the activation of apoptosis and mitigate I/R-induced myocardial injury. In addition, Sal markedly reduced the expression of COX-2 after I/R, indicating that Sal effectively inhibited injury by suppressing COX-2.

NS398, a specific inhibitor of COX-2 [40], is known to play a cardioprotective effect against I/R injury [28], and has been shown to protect against progression of cell apoptosis. However, whether the anti-apoptotic effect of NS398 is linked to ER stress is unclear. We showed that NS398 pretreatment resulted in a distinct decrease of Cleaved caspase 3, indicating that NS398 alleviates apoptosis.

Inhibition of COX2 activity with NS398 consistently decreased the expression level of the components of the COX2 [41-43]. Therefore, detecting the expression of COX2 protein is an effective strategy to verify the effect of NS398 in this study. Consistent with previous studies which showed a close connection between COX-2 and ER stress [44, 45]. Our data showed that NS398 decreased the ER stress level by inhibition of COX-2. Augmentation of GRP78 is recognized as the beginning of ER stress [46], and CHOP is known as the key element of cell death and ER stress-induced apoptosis [47]. Increased CHOP expression and cell death occur during excessive and persistent ER stress. In the present study, the expression of CHOP was significantly decreased after NS398 administration, suggesting that NS398 suppresses ER stress in I/R by inhibiting the expression of CHOP and the ER stress-related signaling pathway. These results were similar to the results of the investigation that celecoxib could significantly reduce the key ER stress proteins BIP and CHOP. They concluded that COX-2 activates ER stress through the BIP/CHOP pathway, further exacerbating lung injury [48]. Furthermore, the suppression of COX-2-

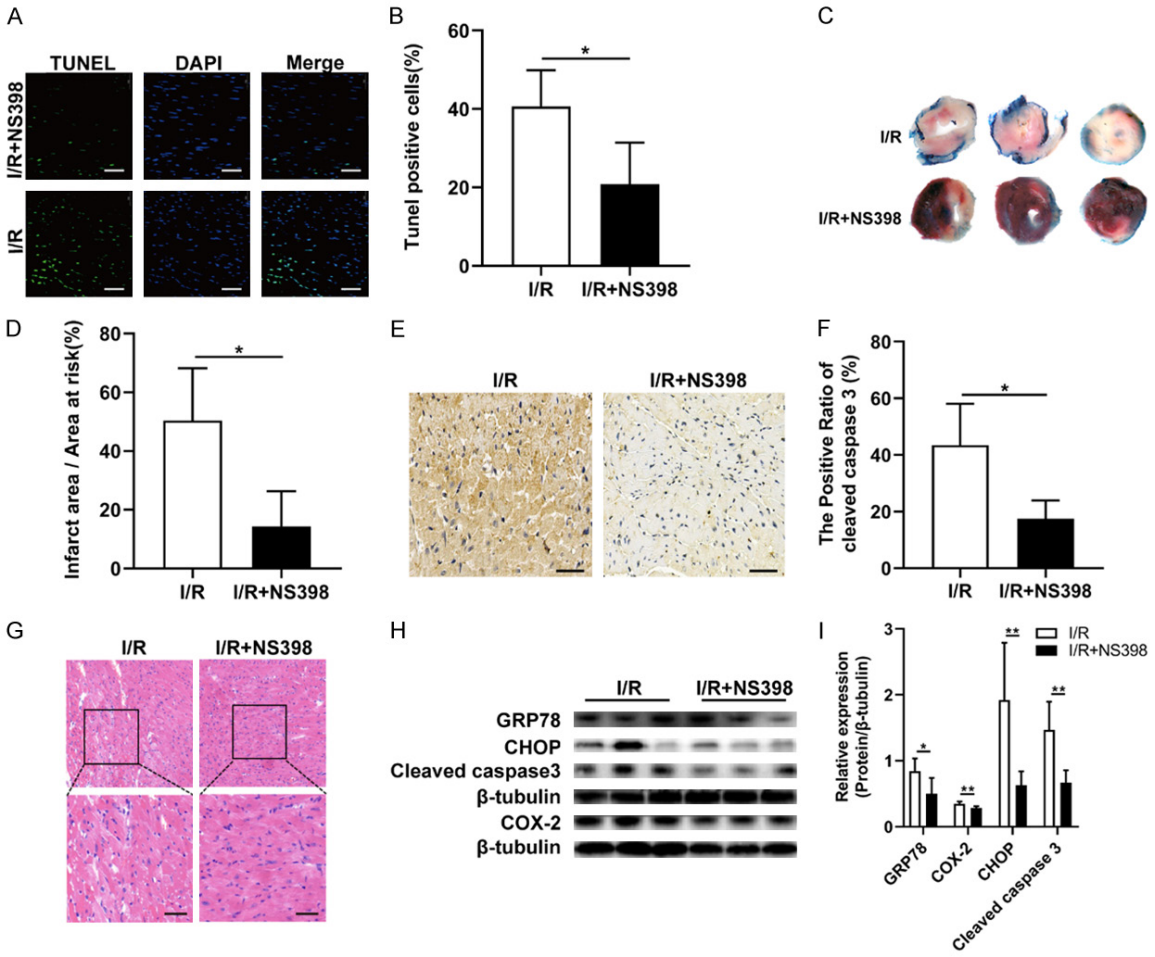

Figure 6. NS398 alleviates myocardial I/R-induced apoptosis through regulating ER stress in vivo. A, B. TUNEL assay (n=4), Scale bar: 50 μm; C, D. Evans blue-TTC dual staining; E, F. Immunohistochemistry (n=4), Scale bar: 50 μm; G. HE staining (n=4), Scale bar: 50 μm; H, I. Western blot analysis of GRP78, CHOP, Cleaved caspase 3, and COX-2 proteins in myocardial tissue (n=4). Data presented as mean ± standard deviation. *P<0.05, **P<0.01.

mediated PI3K/Akt pathway with celecoxib successfully down-regulated ER stress in hepatocellular carcinoma cells [45]. Therapeutic administration of celecoxib effectively reduces hepatic apoptosis in thioacetamide-induced cirrhotic rats. The mechanism of action may be attributed to the suppression of CHOP expression, which subsequently inhibits ER stress [49]. A limitation of this study is that it only explores the interaction between COX-2 and ER stress, which leads to apoptosis and aggravates myocardial I/R injury. Further explorations are required for the complex regulatory mechanism between COX-2 and ER stress.

Conclusion

Our research reveals that I/R can induce apoptosis by activating the ER stress and upregulating the COX-2. ER stress may be related to COX-2-induced apoptosis, which can be inhibited by specific COX-2 inhibitor NS398. Sal significantly decreased the expression of COX-2 after I/R, indicating that Sal can suppress cell injury and apoptosis by inhibiting COX-2 (**Figure 7**). Although further studies are required to assess the efficacy of COX-2 and ER stress as therapeutic targets for AMI, our results highlight the need to further investigate COX-2 and ER stress-mediated-apoptosis inhibition strategies for myocardial I/R injury.

Acknowledgements

This work was supported by the National Natural Science Foundation of China (82072130 and 81873925 to FHJ). 333 High-level Talent Training Project in Jiangsu Province (BRA2020089 to FHJ).

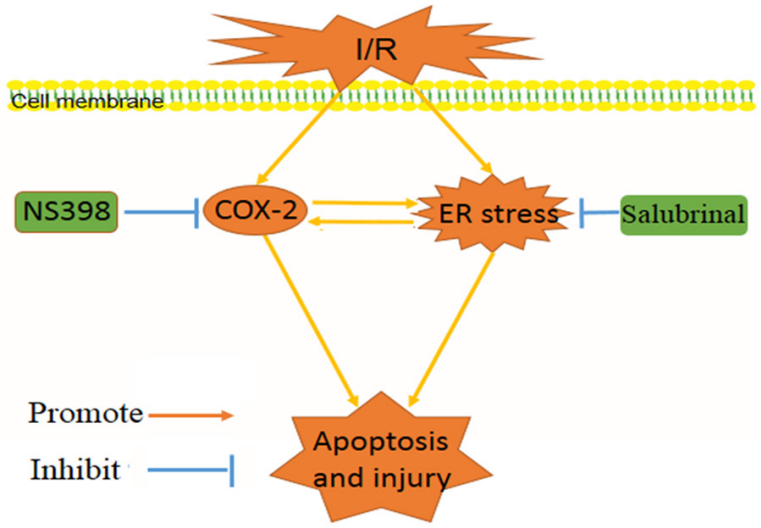

Figure 7. Schematic illustration of the proposed signaling involved in the interaction between COX-2 and ER stress in I/R-induced cardiomyocyte apoptosis. Pretreatment with Sal or NS398 attenuates apoptosis-induced myocardial I/R injury by inhibiting the interaction between COX-2 and ER stress.

Disclosure of conflict of interest

None.

Address correspondence to: Huayue Liu and Fuhai Ji, Department of Anesthesiology, First Affiliated Hospital of Soochow University, No. 899 Pinghai Road, Suzhou 215006, Jiangsu, China. Tel: +86-512-6797-2352; E-mail: docliu.hy@163.com (HYL); jifuhai1968@163.com (FHJ)

References

[1] Ibáñez B, Heusch G, Ovize M and Van de Werf F. Evolving therapies for myocardial ischemia/reperfusion injury. J Am Coll Cardiol 2015; 65: 1454-1471.

[2] Eltzschig HK and Eckle T. Ischemia and reperfusion - from mechanism to translation. Nat Med 2011; 17: 1391-1401.

[3] Peng K, Liu H, Yan B, Meng XW, Song SY, Ji FH and Xia Z. Inhibition of cathepsin S attenuates myocardial ischemia/reperfusion injury by suppressing inflammation and apoptosis. J Cell Physiol 2021; 236: 1309-1320.

[4] Zhang J, Huang L, Shi X, Yang L, Hua F, Ma J, Zhu W, Liu X, Xuan R, Shen Y, Liu J, Lai X and Yu P. Metformin protects against myocardial ischemia-reperfusion injury and cell pyroptosis via AMPK/NLRP3 inflammasome pathway. Aging (Albany NY) 2020; 12: 24270-24287.

[5] Guo X, Hong S, He H, Zeng Y, Chen Y, Mo X, Li J, Li L, Steinmetz R and Liu Q. NFκB promotes oxidative stress-induced necrosis and ischemia/reperfusion injury by inhibiting Nrf2-ARE pathway. Free Radic Biol Med 2020; 159: 125-135.

[6] Wang F, Wang H, Liu X, Yu H, Huang X, Huang W and Wang G. Neuregulin-1 alleviate oxidative stress and mitigate inflammation by suppressing NOX4 and NLRP3/caspase-1 in myocardial ischaemia-reperfusion injury. J Cell Mol Med 2021; 25: 1783-1795.

[7] Xue J, Yan X, Yang Y, Chen M, Wu L, Gou Z, Sun Z, Talabieke S, Zheng Y and Luo D. Connexin 43 dephosphorylation contributes to arrhythmias and cardiomyocyte apoptosis in ischemia/reperfusion hearts. Basic Res Cardiol 2019; 114: 40.

[8] Minami K, Bae S, Uehara H, Zhao C, Lee D, Iske J, Fanger MW, Reder J, Morrison I, Azuma H, Wiens A, Van Keuren E, Houser B, ElKhal A, Kang PM and Tullius SG. Targeting of intragraft reactive oxygen species by APP-103, a novel polymer product, mitigates ischemia/reperfusion injury and promotes the survival of renal transplants. Am J Transplant 2020; 20: 1527-1537.

[9] Yu P, Ma S, Dai X and Cao F. Elabela alleviates myocardial ischemia reperfusion-induced apoptosis, fibrosis and mitochondrial dysfunction through PI3K/AKT signaling. Am J Transl Res 2020; 12: 4467-4477.

[10] Khuanjing T, Palee S, Kerdphoo S, Jaiwongkam T, Anomasiri A, Chattipakorn SC and Chattipakorn N. Donepezil attenuated cardiac ischemia/reperfusion injury through balancing mitochondrial dynamics, mitophagy, and autophagy. Transl Res 2021; 230: 82-97.

[11] Wang N, Ma J, Ma Y, Lu L, Ma C, Qin P, Gao E, Zuo M, Yang J and Yang L. Electroacupuncture pretreatment mitigates myocardial ischemia/reperfusion injury via XBP1/GRP78/Akt pathway. Front Cardiovasc Med 2021; 8: 629547.

[12] Li F, Zhan Z, Qian J, Cao C, Yao W and Wang N. Naringin attenuates rat myocardial ischemia/reperfusion injury via PI3K/Akt pathway-mediated inhibition of apoptosis, oxidative stress and autophagy. Exp Ther Med 2021; 22: 811.

[13] Song Q, Feng YB, Wang L, Shen J, Li Y, Fan C, Wang P and Yu SY. COX-2 inhibition rescues depression-like behaviors via suppressing glial activation, oxidative stress and neuronal apoptosis in rats. Neuropharmacology 2019; 160: 107779.

[14] Salvo F, Antoniazzi S, Duong M, Molimard M, Bazin F, Fourrier-Réglat A, Pariente A and Moore N. Cardiovascular events associated with the long-term use of NSAIDs: a review of randomized controlled trials and observational studies. Expert Opin Drug Saf 2014; 13: 573-585.
[15] Pirlamarla P and Bond RM. FDA labeling of NSAIDs: Review of nonsteroidal anti-inflammatory drugs in cardiovascular disease. Trends Cardiovasc Med 2016; 26: 675-680.
[16] Wang ZF, Gao C, Chen W, Gao Y, Wang HC, Meng Y, Luo CL, Zhang MY, Chen G, Chen XP, Wang T and Tao LY. Salubrinal offers neuroprotection through suppressing endoplasmic reticulum stress, autophagy and apoptosis in a mouse traumatic brain injury model. Neurobiol Learn Mem 2019; 161: 12-25.
[17] Zhao Z, Wu J, Xu H, Zhou C, Han B, Zhu H, Hu Z, Ma Z, Ming Z, Yao Y, Zeng R and Xu G. XJB-5-131 inhibited ferroptosis in tubular epithelial cells after ischemia-reperfusion injury. Cell Death Dis 2020; 11: 629.
[18] Zhang BF, Jiang H, Chen J, Guo X, Li Y, Hu Q and Yang S. Nobiletin ameliorates myocardial ischemia and reperfusion injury by attenuating endoplasmic reticulum stress-associated apoptosis through regulation of the PI3K/AKT signal pathway. Int Immunopharmacol 2019; 73: 98-107.
[19] Sun F, Du J, Li H, Hao S, Zhao G and Lu F. FABP4 inhibitor BMS309403 protects against hypoxia-induced H9c2 cardiomyocyte apoptosis through attenuating endoplasmic reticulum stress. J Cell Mol Med 2020; 24: 11188-11197.
[20] Li W, Li W, Leng Y, Xiong Y, Xia Z. Ferroptosis is involved in diabetes myocardial ischemia/reperfusion injury through endoplasmic reticulum stress. DNA Cell Biol 2020; 39: 210-225.
[21] Yang CH, Qi WL, Zhao CW, Cai WJ, Gong Q, Niu JY, Zhao WH and Xu L. Parecoxib prevents nucleus pulposus cells apoptosis by suppressing endoplasmic reticulum stress. Eur Rev Med Pharmacol Sci 2020; 24: 11295-11304.
[22] Luo B, Lin Y, Jiang S, Huang L, Yao H, Zhuang Q, Zhao R, Liu H, He C and Lin Z. Endoplasmic reticulum stress eIF2α-ATF4 pathway-mediated cyclooxygenase-2 induction regulates cadmium-induced autophagy in kidney. Cell Death Dis 2016; 7: e2251.
[23] Cho HK, Cheong KJ, Kim HY and Cheong J. Endoplasmic reticulum stress induced by hepatitis B virus X protein enhances cyclo-oxygenase 2 expression via activating transcription factor 4. Biochem J 2011; 435: 431-439.
[24] Han M, Gao H, Xie J, Yuan Y, Yuan Q, Gao M, Liu K, Chen X, Han Y and Han Z. Hispidulin induces ER stress-mediated apoptosis in human hepatocellular carcinoma cells in vitro and in vivo by activating AMPK signaling pathway. Acta Pharmacol Sin 2019; 40: 666-676.
[25] Bian M, He J, Jin H, Lian N, Shao J, Guo Q, Wang S, Zhang F and Zheng S. Oroxylin A induces apoptosis of activated hepatic stellate cells through endoplasmic reticulum stress. Apoptosis 2019; 24: 905-920.
[26] Song C, Liu L, Chen J, Hu Y, Li J, Wang B, Bellusci S, Chen C and Dong N. Evidence for the critical role of the PI3K signaling pathway in particulate matter-induced dysregulation of the inflammatory mediators COX-2/PGE and the associated epithelial barrier protein Filaggrin in the bronchial epithelium. Cell Biol Toxicol 2020; 36: 301-313.
[27] Martínez-Torres S, Cutando L, Pastor A, Kato A, Sakimura K, de la Torre R, Valjent E, Maldonado R, Kano M and Ozaita A. Monoacylglycerol lipase blockade impairs fine motor coordination and triggers cerebellar neuroinflammation through cyclooxygenase-2. Brain Behav Immun 2019; 81: 399-409.
[28] Pang L, Cai Y, Tang E, Yan D, Kosuru R, Li H, Irwin M, Ma H and Xia Z. viaCox-2 inhibition protects against hypoxia/reoxygenation-induced cardiomyocyte apoptosis akt-dependent enhancement of iNOS expression. Oxid Med Cell Longev 2016; 2016: 3453059.
[29] Jin T, Lin J, Gong Y, Bi X, Hu S, Lv Q, Chen J, Li X, Chen J, Zhang W, Wang M and Fu G. iPLAβ contributes to ER stress-induced apoptosis during myocardial ischemia/reperfusion injury. Cells 2021; 10: 1446.
[30] Chen C, Lu C, He D, Na N, Wu Y, Luo Z and Huang F. Inhibition of HMGB1 alleviates myocardial ischemia/reperfusion injury in diabetic mice via suppressing autophagy. Microvasc Res 2021; 138: 104204.
[31] Li RJ, He KL, Li X, Wang LL, Liu CL and He YY. Salubrinal protects cardiomyocytes against apoptosis in a rat myocardial infarction model via suppressing the dephosphorylation of eukaryotic translation initiation factor 2α. Mol Med Rep 2015; 12: 1043-1049.
[32] Zhang J, Wang Y, Ju M, Song J, Zheng Y, Lin S, Zhu D, Wen L, Zhong M, Pan S and Yang G. Neuroprotective effect of the inhibitor salubrinal after cardiac arrest in a rodent model. Oxid Med Cell Longev 2020; 2020: 7468738.
[33] Jiang X, Shi E, Nakajima Y, Sato S, Ohno K and Yue H. Cyclooxygenase-1 mediates the final stage of morphine-induced delayed cardioprotection in concert with cyclooxygenase-2. J Am Coll Cardiol 2005; 45: 1707-1715.
[34] Yang Y, Wang H, Song N, Jiang Y, Zhang J, Meng X, Feng X, Liu H, Peng K and Ji F. Dexmedetomidine attenuates ischemia/reperfusion-induced myocardial inflammation and apopto-

sis through inhibiting endoplasmic reticulum stress signaling. J Inflamm Res 2021; 14: 1217-1233.
[35] Yuan M, Meng XW, Ma J, Liu H, Song SY, Chen QC, Liu HY, Zhang J, Song N, Ji FH and Peng K. Dexmedetomidine protects H9c2 cardiomyocytes against oxygen-glucose deprivation/reoxygenation-induced intracellular calcium overload and apoptosis through regulating FKBP12.6/RyR2 signaling. Drug Des Devel Ther 2019; 13: 3137-3149.
[36] Li W, Li W, Leng Y, Xiong Y and Xia Z. Ferroptosis is involved in diabetes myocardial ischemia/reperfusion injury through endoplasmic reticulum stress. DNA Cell Biol 2020; 39: 210-225.
[37] Pang L, Cai Y, Tang EH, Yan D, Kosuru R, Li H, Irwin MG, Ma H and Xia Z. Cox-2 inhibition protects against hypoxia/reoxygenation-induced cardiomyocyte apoptosis via akt-dependent enhancement of iNOS expression. Oxid Med Cell Longev 2016; 2016: 3453059.
[38] Ruan Y, Zeng J, Jin Q, Chu M, Ji K, Wang Z and Li L. Endoplasmic reticulum stress serves an important role in cardiac ischemia/reperfusion injury (Review). Exp Ther Med 2020; 20: 268.
[39] Jin T, Lin J, Gong Y, Bi X, Hu S, Lv Q, Chen J, Li X, Chen J, Zhang W, Wang M and Fu G. iPLA(2) β Contributes to ER stress-induced apoptosis during myocardial ischemia/reperfusion injury. Cells 2021; 10: 1446.
[40] Stachowicz K, Bobula B and Tokarski K. NS398, a cyclooxygenase-2 inhibitor, reverses memory performance disrupted by imipramine in C57Bl/6J mice. Brain Res 2020; 1734: 146741.
[41] Kuang C, Zhu Y, Guan Y, Xia J, Ouyang J, Liu G, Hao M, Liu J, Guo J, Zhang W, Feng X, Li X, Zhang J, Wu X, Xu H, Li G, Xie L, Fan S, Qiu L and Zhou W. COX2 confers bone marrow stromal cells to promoting TNFα/TNFR1β-mediated myeloma cell growth and adhesion. Cell Oncol (Dordr) 2021; 44: 643-659.
[42] Galamb O, Spisák S, Sipos F, Tóth K, Solymosi N, Wichmann B, Krenács T, Valcz G, Tulassay Z and Molnár B. Reversal of gene expression changes in the colorectal normal-adenoma pathway by NS398 selective COX2 inhibitor. Br J Cancer 2010; 102: 765-773.
[43] Chen L, Ji X, Wang M, Liao X, Liang C, Tang J, Wen Z, Dominique F and Li Z. Involvement of TLR4 signaling regulated-COX2/PGE2 axis in liver fibrosis induced by Schistosoma japonicum infection. Parasit Vectors 2021; 14: 279.
[44] Chen P, Geng N, Zhou D, Zhu Y, Xu Y, Liu K, Liu Y and Liu J. The regulatory role of COX-2 in the interaction between Cr(VI)-induced endoplasmic reticulum stress and autophagy in DF-1 cells. Ecotoxicol Environ Saf 2019; 170: 112-119.
[45] Yang MY, Wu CH, Hung TW and Wang CJ. Endoplasmic reticulum stress-induced resistance to doxorubicin is reversed by mulberry leaf polyphenol extract in hepatocellular carcinoma through inhibition of COX-2. Antioxidants (Basel) 2019; 9: 26.
[46] Elfiky AA, Baghdady AM, Ali SA and Ahmed MI. GRP78 targeting: Hitting two birds with a stone. Life Sci 2020; 260: 118317.
[47] Olivares-Silva F, Espitia-Corredor J, Letelier A, Vivar R, Parra-Flores P, Olmedo I, Montenegro J, Pardo-Jiménez V and Díaz-Araya G. TGF-β1 decreases CHOP expression and prevents cardiac fibroblast apoptosis induced by endoplasmic reticulum stress. Toxicol In Vitro 2021; 70: 105041.
[48] Choo-Wing R, Syed MA, Harijith A, Bowen B, Pryhuber G, Janér C, Andersson S, Homer RJ and Bhandari V. Hyperoxia and interferon-γ-induced injury in developing lungs occur via cyclooxygenase-2 and the endoplasmic reticulum stress-dependent pathway. Am J Respir Cell Mol Biol 2013; 48: 749-757.
[49] Su W, Tai Y, Tang SH, Ye YT, Zhao C, Gao JH, Tuo BG and Tang CW. Celecoxib attenuates hepatocyte apoptosis by inhibiting endoplasmic reticulum stress in thioacetamide-induced cirrhotic rats. World J Gastroenterol 2020; 26: 4094-4107.